A 3-D Finite Element Formulation for Calculating Meissner Currents in Superconductors

Christophe Cordier, Stéphane Flament, and Christian Dubuc

***Abstract*—A three-dimensional (3-D) finite element formulation for calculating Meissner currents in superconductors is presented. The authors have chosen a magnetic vector potential formulation, which also enables them to simulate ferromagnetic shielding. The equations are written so that the problem can be solved by the use of a conjugate gradient algorithm without preconditioning. Numerical results on normal–superconductor junctions and on superconducting lines are compared with analytical solutions.**

***Index Terms*— Finite element method, modeling, simulation, superconductor.**

I. Introduction

PERFORMANCES of superconducting magnetometers such as superconducting quantum interference device (SQUID) or Josephson Fraunhofer Magnetometer (JFM) can be improved by optimizing the design of these devices. The relative complexity of the thin film structures actually used in our systems rules out the possibility of finding any analytical solution.

We propose in this paper to solve Maxwell's equations, by taking into account the supercurrent and by using the finite element method (FEM). Our aim is to study superconductors in the Meissner state, under the effect of various magnetic excitations.

II. Problem Equations

We consider the quasi-stationary state and thus we write the Maxwell's equations relating the magnetic flux density B to the current density J as follows:

$$\nabla \times B = \mu_0 J \tag{1}$$

$$\nabla \cdot B = 0. \tag{2}$$

The behavior of the Cooper pairs is determined by a macroscopic complex wavefunction [1]

$$\Psi(r,t) = \sqrt{n^*}\exp[i\theta(r,t)] \tag{3}$$

where n^* is the local density of Cooper pairs and $\theta(r,t)$ is a real number representing the phase.

Writing the wavefunction in the Schrödinger's equation [2], we find the density of supercurrent J_s

$$J_s = \frac{1}{\mu_0 \lambda_L^2}\left(-A + \frac{\Phi_0}{2\pi}\nabla\theta\right) \tag{4}$$

Manuscript received July 24, 1998; revised December 4, 1998.

The authors are with GREYC–CNRS UPRES A 6072, ISMRA et Université de Caen, 14000 Caen Cedex, France.

Publisher Item Identifier S 1051-8223(99)03714-8.

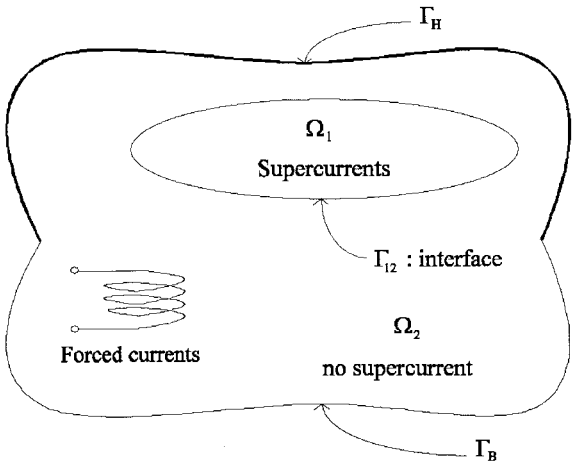

Fig. 1. Description of a supercurrent problem.

where λ_L and Φ_0 stand, respectively, for the London penetration depth and the flux quantum, and the magnetic vector potential A is defined by $B = \nabla \times A$. Notice that by taking the curl of (4) we get the second London equation $\nabla \times J_S + (1/\mu_0\lambda_L^2)B = 0$.

A typical supercurrent problem is depicted in Fig. 1. It consists of a superconducting region (Ω_1) surrounded by a region Ω_2 without any supercurrent but which may contain forced currents. The union of Ω_1 and Ω_2 forms the whole space. We shall distinguish the following boundary conditions which define three types of boundaries:

1) Γ_B where the normal component of flux density is equal to zero;
2) Γ_H where the tangential component of magnetic field is set;
3) Γ_{12} the interface between Ω_1 and Ω_2 where flux density is continuous and the normal component of supercurrent is null.

Thus

$$B \cdot n = 0 \qquad \text{on } \Gamma_B \tag{5}$$

$$H \times n = V \qquad \text{on } \Gamma_H \tag{6}$$

$$\left.\begin{aligned} B_1 \cdot n_1 + B_2 \cdot n_2 &= 0 \\ H_1 \times n_1 + H_2 \times n_2 &= 0 \\ J \cdot n = J_s \cdot n &= 0 \end{aligned}\right\} \quad \text{on } \Gamma_{12} \tag{7, 8, 9}$$

where indexes 1 and 2 refer, respectively, to regions Ω_1 and Ω_2, and V is a vector which can be null.

Knowing that $B = \mu_0 H$ in the superconducting material and in Ω_2, the previous boundary conditions become

$$B \cdot n = 0 \quad \text{on } \Gamma_B \tag{10}$$
$$B \times n = V \quad \text{on } \Gamma_H \tag{11}$$
$$\left.\begin{aligned} B_1 \cdot n_1 + B_2 \cdot n_2 &= 0 \\ B_1 \times n_1 + B_2 \times n_2 &= 0 \\ J \cdot n = J_s \cdot n &= 0 \end{aligned}\right\} \quad \text{on } \Gamma_{12}. \tag{12--14}$$

Nodal FEM requires continuous unknowns, therefore two different sets of unknowns can be chosen. If we choose B, we have to take into account system I

$$I \begin{cases} \left.\begin{aligned} \nabla \times B - \mu_0 J_s &= 0 \\ \nabla \times J_s + \frac{1}{\mu_0 \lambda_L^2} B &= 0 \\ \nabla \cdot B &= 0 \end{aligned}\right\} & \text{In } \Omega_1 \quad (15)\text{--}(17) \\ \left.\begin{aligned} \nabla \times B &= \mu_0 J \\ \nabla \cdot B &= 0 \end{aligned}\right\} & \text{In } \Omega_2 \quad (18)\text{--}(19) \\ B \cdot n = 0 & \text{On } \Gamma_B \quad (20) \\ B \times n = V & \text{On } \Gamma_H \quad (21) \\ \left.\begin{aligned} B_1 \cdot n_1 + B_2 \cdot n_2 &= 0 \\ B_1 \times n_1 + B_2 \times n_2 &= 0 \\ J \cdot n = J_s \cdot n &= 0 \end{aligned}\right\} & \text{On } \Gamma_{12}. \quad (22)\text{--}(24) \end{cases}$$

By analogy with the work of Biro *et al.* in the field of eddy currents [3], (15)–(23) uniquely define B, provided that Γ_B and Γ_H are simply connected. If we choose A and θ we have to solve system II

$$II \begin{cases} \nabla \times \nabla \times A + \frac{1}{\lambda_L^2} A - \frac{\Phi_0}{2\pi\lambda_L^2} \nabla\theta = 0 & \text{In } \Omega_1 \quad (25) \\ \nabla \times \nabla \times A = \mu_0 J & \text{In } \Omega_2 \quad (26) \\ \nabla \times A \cdot n = 0 & \text{On } \Gamma_B \quad (27) \\ \nabla \times A \times n = V & \text{On } \Gamma_H \quad (28) \\ \left.\begin{aligned} \nabla \times A_1 \cdot n_1 + \nabla \times A_2 \cdot n_2 &= 0 \\ \nabla \times A_1 \times n_1 + \nabla \times A_2 \times n_2 &= 0 \\ J \cdot n = J_s \cdot n &= 0 \end{aligned}\right\} & \text{On } \Gamma_{12}. \quad (29)\text{--}(31) \end{cases}$$

System II is equivalent to system I, so (25)–(30) determine $\nabla \times A$ but not A.

The choice of B is unadapted for simulating ferromagnetic shielding in the vicinity of our superconducting structures since at the air-ferromagnetic interface, the tangential component of B is not continuous. Therefore, we turned our attention to system II. For the sake of clearness we have not detailed in this paper the FEM formulation for cases including ferromagnetic region.

III. Finite Element Formulation

We now examine the conditions ensuring the uniqueness of the magnetic vector potential A and of the phase θ.

If A and θ are solutions of (25)–(30), then A_1 and θ_1 defined by

$$A_1 = A + \nabla u \tag{32}$$
$$\theta_1 = \theta + v \tag{33}$$

where v is a constant, are also solutions.

In order to remove the ambiguity on θ, we just have to fix the value of θ at one point in Ω_1.

One way to obtain the uniqueness of A is to enforce the Coulomb gauge $\nabla \cdot A = 0$ and to add necessary conditions on Γ_B and Γ_H which are as follows:

$$n \times A = 0 \text{ on } \Gamma_B, \text{ which replace (27) (see Morisue [4])} \tag{34}$$
$$n \cdot A = 0 \text{ on } \Gamma_H, \text{ which do not affect (28)} \tag{35}$$

This gauge is classically enforced by adding to (25) and (26) a term of the form $-p\nabla(\nabla \cdot A)$ [5], where p is a constant chosen empirically. Because of this term, condition (31) is no longer a consequence of (25). To impose (31), $\nabla \cdot J_s$ must be set to zero in Ω_1. Consequently, by taking the divergence of (25) and (26), we have $\nabla^2(p\nabla \cdot A) = 0$ in Ω_1 and Ω_2. This equation implies additional boundary conditions (40) and (45) [6].

Knowing that continuity of A ensures the satisfaction of (29), the system of differential equations finally becomes as shown in (36)–(46), at the bottom of the page.

Boundary conditions (39) and (42) are Dirichlet conditions and (40), (41), and (46) are Neumann conditions.

$$\left.\begin{aligned} \nabla \times \nabla \times A - p\nabla(\nabla \cdot A) + \frac{1}{\lambda_L^2} A - \frac{\Phi_0}{2\pi\lambda_L^2} \nabla\theta &= 0 \\ \nabla \cdot \left(-\frac{1}{\mu_0 \lambda_L^2} A + \frac{\Phi_0}{2\pi\mu_0\lambda_L^2} \nabla\theta \right) &= 0 \end{aligned}\right\} \text{ In } \Omega_1 \quad (36)\text{--}(37)$$
$$\nabla \times \nabla \times A - p\nabla(\nabla \cdot A) = \mu_0 J \quad \text{In } \Omega_2 \tag{38}$$
$$\left.\begin{aligned} n \times A &= 0 \\ p\nabla \cdot A &= 0 \end{aligned}\right\} \text{ On } \Gamma_B \quad (39)\text{--}(40)$$
$$\left.\begin{aligned} \nabla \times A \times n &= V \\ n \cdot A &= 0 \end{aligned}\right\} \text{ On } \Gamma_H \quad (41)\text{--}(42)$$
$$\left.\begin{aligned} A_1 &= A_2 \\ \nabla \times A_1 \times n_1 + \nabla \times A_2 \times n_2 &= 0 \\ p_1 \nabla \cdot A_1 - p_2 \nabla \cdot A_2 &= 0 \\ n \cdot \left(-\frac{1}{\mu_0 \lambda_L^2} A + \frac{\Phi_0}{2\pi\mu_0\lambda_L^2} \nabla\theta \right) &= 0 \end{aligned}\right\} \text{ On } \Gamma_{12} \quad (43)\text{--}(46)$$

IV. Finite Element Discretization

In the finite element approximation the region to study is decomposed in small geometrical elements which form the mesh. The potentials A and θ are approximated with their values A_j and θ_j at node j and with the shape functions α_j associated to node j

$$A=\sum_{j=1}^{Nn}\alpha_j[I_3]A_j \quad \text{and} \quad \theta=\sum_{j=1}^{Nn}\alpha_j\theta_j$$

where N_n is the total number of nodes of the mesh and I_3 is the identity matrix of rank 3.

The shape function α_j associated to node j is equal to one at node j and zero at any other node.

The Galerkin weighted residual method (see Zienkiewicz [7]) is used to discretize (36)–(38). In this case the weighting factors w_i and W_i are written with the shape functions $w_i=\alpha_i$ and $W_i=\alpha_i[I_3]$ so that

$$A=\sum_{j=1}^{Nn}W_jA_j \tag{47}$$

and

$$\theta=\sum_{j=1}^{Nn}w_j\theta_j. \tag{48}$$

It is shown that finding A and θ as solutions of (36)–(38) is equivalent to finding A and θ satisfying at each node i [8]

$$\int_{\Omega_1}W_i\cdot\left[\nabla\times\nu\nabla\times A-p\nu\nabla(\nabla\cdot A)+\frac{1}{\lambda_L^2}A-\frac{\Phi_0}{2\pi\lambda_L^2}\nabla\theta\right]d\Omega=0 \tag{49}$$

$$\int_{\Omega_1}w_i\nabla\cdot\left(-\frac{1}{\mu_0\lambda_L^2}A+\frac{\Phi_0}{2\pi\mu_0\lambda_L^2}\nabla\theta\right)d\Omega=0 \tag{50}$$

$$\int_{\Omega_2}W_i\cdot[\nabla\times\nu\nabla\times A-p\nu\nabla(\nabla\cdot A)]\,d\Omega=0. \tag{51}$$

Using Green's theorem and vector identities we can reduce the differentiation degree in the following equations:

$$\int_{\Omega_1}\left[\nabla\times W_i\cdot\nu\nabla\times A+p\nu\nabla\cdot W_i\nabla\cdot A+\frac{1}{\lambda_L^2}W_i\cdot A-\frac{\Phi_0}{2\pi\lambda_L^2}W_i\cdot\nabla\theta\right]d\Omega \tag{52}$$

$$-\int_{\Gamma_{12}}W_i\cdot[\nu\nabla\times A_1\times n_1]\,d\Gamma-\int_{\Gamma_{12}}W_i\cdot n(p_1\nu\nabla\cdot A_1)\,d\Gamma=0 \tag{53}$$

$$\int_{\Gamma_1}\left[-\frac{1}{\mu_0\lambda_L^2}\nabla W_i\cdot A+\frac{\Phi_0}{2\pi\mu_0\lambda_L^2}\nabla w_i\cdot\nabla\theta\right]d\Omega-\int_{\Gamma_{12}}w_in\cdot\left[-\frac{1}{\mu_0\lambda_L^2}A+\frac{\Phi_0}{2\pi\mu_0\lambda_L^2}\nabla\theta\right]d\Gamma=0. \tag{54}$$

The shape functions at the nodes belonging to Γ_B and Γ_H are not used as weighting functions because of Dirichlet boundary conditions (39) and (42), so that we have

$$n\times W_i=0 \qquad \text{on } \Gamma_B \tag{55}$$

$$n\cdot W_i=0 \qquad \text{on } \Gamma_H. \tag{56}$$

According to the boundary conditions (40), (46), (55), and (56) the third, fifth, and sixth surface integral in (54), as well as the surface integral in (53), vanish. By adding (52)–(54) and according to (44) and (45) the surface integrals on Γ_{12} cancel each other.

Consequently we get

$$\int_{\Omega_1}\left[\nabla\times W_i\cdot\nu\nabla\times A+p\nu\nabla\cdot W_i\nabla\cdot A+\frac{1}{\lambda_L^2}W_i\cdot A-\frac{\Phi_0}{2\pi\lambda_L^2}W_i\cdot\nabla\theta\right]d\Omega=0 \tag{57}$$

$$\int_{\Omega_1}\left[-\frac{1}{\mu_0\lambda_L^2}\nabla w_i\cdot A+\frac{\Phi_0}{2\pi\mu_0\lambda_L^2}\nabla w_i\cdot\nabla\theta\right]d\Omega=0 \tag{58}$$

$$\int_{\Omega_2}[\nabla\times W_i\cdot\nu\nabla\times A+p\nu\nabla\cdot W_i\nabla\cdot A]\,d\Omega=\int_{\Gamma_H}W_i\cdot[\nu\nabla\times A\times n]\,d\Gamma. \tag{59}$$

We then have to optimize the numerical solving of the resulting matrix formulation. A rough evaluation of the different terms contained in the final matrix shows that it is badly conditioned [9]. Indeed, the mesh size and λ_L are about a micrometer and Φ_0 is equal to 2.10^{-15} Wb. To remedy this situation, we multiply (58) by $\mu_0\lambda_L$ and write

$$\Phi=\frac{\Phi_0}{2\pi\lambda_L}\theta\left(\text{respectively at each node } i\,\Phi_i=\frac{\Phi_0}{2\pi\lambda_L}\theta_i\right) \tag{60}$$

which leads to the equations

$$\int_{\Omega_1}\left[\nabla\times W_i\cdot\nu\nabla\times A+p\nu\nabla\cdot W_i\nabla\cdot A+\frac{1}{\lambda_L^2}W_i\cdot A-\frac{1}{\lambda_L}W_i\cdot\nabla\Theta\right]d\Omega=0 \tag{61}$$

$$\int_{\Omega_1}\left[-\frac{1}{\lambda_L}\nabla w_i\cdot A+\nabla w_i\cdot\nabla\Theta\right]d\Omega=0 \tag{62}$$

$$\int_{\Omega_2}[\nabla\times W_i\cdot\nu\nabla\times A+p\nu\nabla\cdot W_i\nabla\cdot A]\,d\Omega=\int_{\Gamma_H}W_i\cdot[\nu\nabla\times A\times n]\,d\Gamma. \tag{63}$$

Writing the approximation of A (47) and of Θ [(48) and (60)] in (61)–(63), and permuting the integration and summation symbols we get

$$\sum_{j=1}^{Nn}\left[\int_{\Omega_1}\left[\nabla\times W_i\cdot\nu\nabla\times W_j+p\nu\nabla\cdot W_i\nabla\cdot W_j+\frac{1}{\lambda_L^2}W_i\cdot W_j\right]d\Omega\right][A_j]+\sum_{j=1}^{Nn}\left[\int_{\Omega_1}\left[-\frac{1}{\lambda_L}W_i\cdot\nabla w_j\right]d\Omega\right][\Theta_j]=0 \tag{64}$$

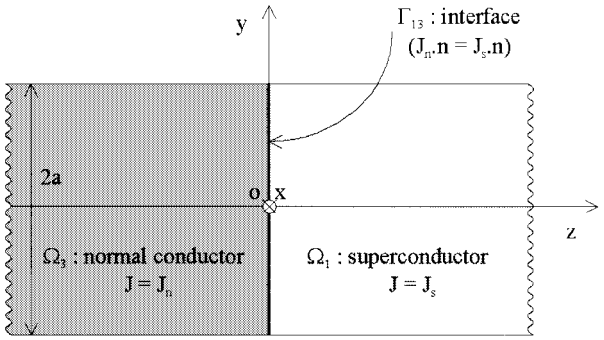

Fig. 2. Normal–superconductor junction. Both normal and superconducting lines are semi-infinite along z. The thickness is in the x-direction. The current density in the normal region (J_n) is uniformly distributed.

$$\sum_{j=1}^{Nn}\left[\int_{\Omega_1}\left[-\frac{1}{\lambda_L}\nabla w_i\cdot W_j\right]d\Omega\right][A_j] + \sum_{j=1}^{Nn}\left[\int_{\Omega_1}[\nabla w_i\cdot\nabla w_j]\,d\Omega\right][\Theta_j]=0 \tag{65}$$

$$\sum_{j=1}^{Nn}\left[\int_{\Omega_2}[\nabla\times W_i\cdot\nabla\times W_j+p\nabla\cdot W_i\nabla\cdot W_j]\,d\Omega\right]\cdot[A_j]=\left[\int_{\Gamma_H}[W_i\cdot V]\,d\Gamma\right]. \tag{66}$$

We see that (64)–(66) form a symmetrical linear system composed of $4N_n$ equations with 4-Nn unknowns. The resulting system is well conditioned when p is chosen equal to unity. So a conjugate gradient algorithm, with no preconditioning, is therefore expected to solve it.

V. Numerical Tests

Up to now, no test problem has been built in the field of superconductor simulation. Furthermore, the validation of the currents and fields distributions through experimental devices is rather difficult. So, we will validate in this preliminary paper the $A-\Theta$ formulation by computing supercurrent density in two different configurations made up of a superconducting line. In each case the supercurrent is injected in the superconducting line Ω_1 thanks to a normal line Ω_3 containing normal forced currents J_n, which are uniformly distributed (see Fig. 2).

Therefore, another type of boundary Γ_{13} follows, representing the contact surface between normal and superconducting region. Boundary conditions on Γ_{13} are the same as those on Γ_{12} [(43)–(46)] except that $J_s\cdot n=0$ must be replaced by $J_s\cdot n=J_n\cdot n$, which explains the continuity of the normal component of the total current density. Then conditions on Γ_{13} are

$$\left.\begin{aligned} A_2&=A_3 &(67)\\ \nabla\times A_2\times n_2+\nabla\times A_3\times n_3&=0 &(68)\\ p_2\nabla\cdot A_2-p_3\nabla\cdot A_3&=0 &(69)\\ J_s\cdot n&=J_n\cdot n &(70)\end{aligned}\right\}\ \text{on } \Gamma_{13}.$$

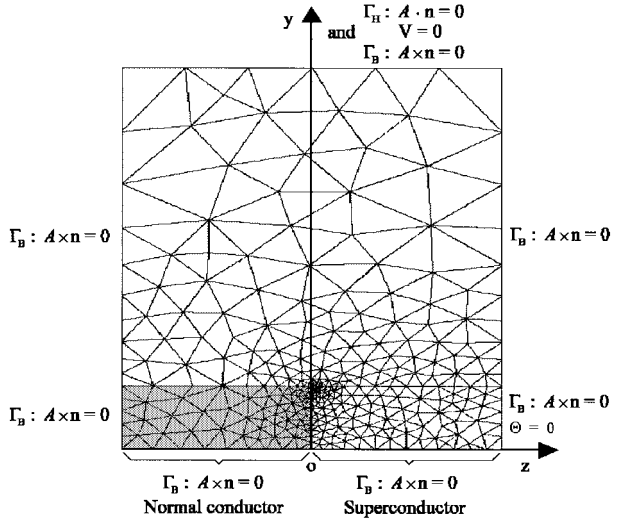

Fig. 3. Meshing of the normal–superconductor junction.

We must modify (62) to get

$$\int_{\Omega_1}\left[-\frac{1}{\lambda_L}\nabla w_i\cdot A+\nabla w_i\cdot\nabla\Theta\right]d\Omega=\int_{\Gamma_{13}}w_i[\mu_0\lambda_L J_s\cdot n]\,d\Gamma. \tag{71}$$

The set of equations with their boundary conditions leads to

$$\int_{\Omega_3}[\nabla\times W_i\cdot\nabla\times A+p\nabla\cdot W_i\nabla\cdot A]\,d\Omega=\int_{\Omega_3}W_i\cdot[\mu_0 J_n]\,d\Gamma. \tag{72}$$

Notice that all integrals on Γ_{13} which normally appear in (61) and (72) are null for the same reasons which made all integrals on Γ_{12} in (52) and (54) null.

The two cases simulated in this paper are constituted of a semi-infinite normal line connected to a semi-infinite superconducting line. As illustrated in Fig. 2 the thickness, the width, and the length of the line are, respectively, along the x-axis, the y-axis and the z-axis.

We first calculate supercurrents in the neighborhood of a normal–superconductor junction of infinite thickness. In the normal conductor, the current density J_n is constant.

The problem was treated in a plane with second-order triangle elements. Fig. 3 shows the region where the numerical calculation was done and presents the finite element meshing used. Boundary conditions are also given.

The results obtained with $2a=2$ μm and $\lambda_L=0.2$ μm are shown in Fig. 4. We note that they are in a very good agreement with the analytical solution [10].

We then consider as a second test configuration the case of a thin superconducting line. We propose to evaluate the current flow in the line far from the interface Γ_{13}, where the calculated current density is z-independent, and compare it with the analytical results of Lee *et al.* [11] given for infinite lines.

A 3-D meshing with second-order tetrahedral elements is done. In Fig. 5 we give numerical results for a line which

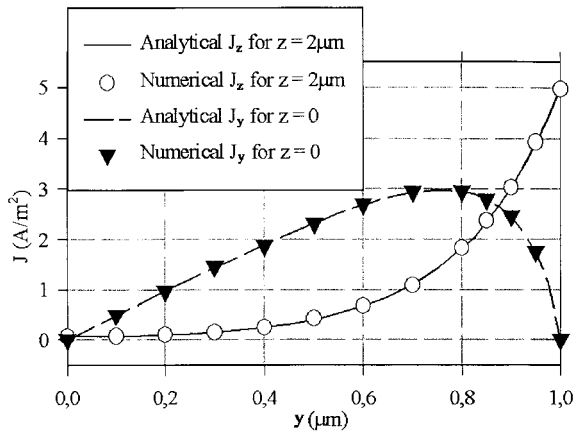

Fig. 4. Analytical [10] and numerical supercurrent density distribution in the superconducting region of Fig. 2 at $z = 2\ \mu$m ($J_y \approx 0$) and at $z = 0$ ($J_z = 1$ A/m^2) ($2a = 2\ \mu$m, $\lambda_L = 2\ \mu$m, $J_n \cdot n = 1$).

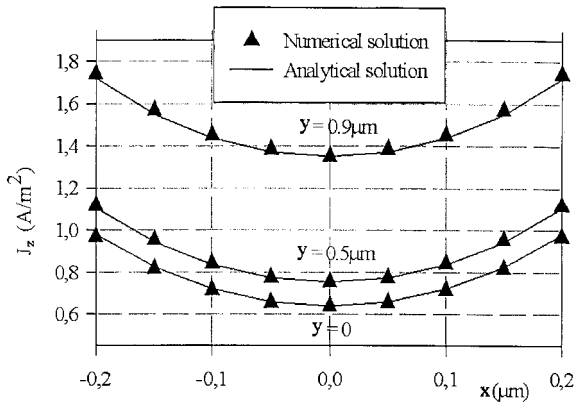

Fig. 5. Analytical [11] and numerical supercurrent density distributions through the thickness of a semi-infinite superconducting line for $y = 0$, $y = 0.5\ \mu$m, and $y = 0.9\ \mu$m. The origin of coordinates is the same as for Fig. 2. The thickness is equal to $2t$ and the distance y is large enough to get $J_y = 0$ ($2a = 2\ \mu$m, $\lambda_L = 2\ \mu$m, $2t = 2\ \mu$m, $J_n \cdot n = 1$).

thickness is twice as the London penetration depth. We see that the analytical formula fits very well the numerical solution.

As predicted all numerical results were obtained by using a conjugate gradient algorithm without preconditioning.

VI. Conclusion

A 3-D finite element formulation for solving Meissner current problems has been presented. We paid particular attention to this formulation so that conjugate gradient algorithm without preconditioning can be used. We have also given conditions under which the magnetic vector potential A and the phase θ are unique.

Numerical results on normal–superconductor junctions and on superconducting lines have been confronted to analytical solutions with success. Our method gives a precious tool to study the behavior of superconducting devices, and it will be applied to more complex designs (see for example [12]–[14]).

It should be noted that our formulation allows us to simulate multiply connected regions provided that the fluxoid is equal to zero. Further work is in progress to surmount this restriction.

References

[1] P. G. De Gennes, *Superconductivity of Metals and Alloys*. New York: W. A. Benjamin, 1966.
[2] T. P. Orlando and K. A. Delin, *Foundations of Applied Superconductivity*. Reading, MA: Addison Wesley, 1991.
[3] O. Biro and K. Preis, "On the use of magnetic vector potential in the finite element analysis of the three-dimensional eddy currents," *IEEE Trans. Magn.*, vol. 25, pp. 3145–3159, 1989.
[4] T. Morisue, "A new formulation of the magnetic vector potential method in 3-D multiply connected regions," *IEEE Trans. Magn.*, vol. 24, pp. 110–113, Jan. 1988.
[5] J. L. Coulomb, Ph.D. dissertation, INP Grenoble, 1981.
[6] D. Albertz, S. Dapen, and G. Henneberger, "Calculation of the 3D nonlinear eddy current field in moving conductors and its application to braking system," *IEEE Trans. Magn.*, vol. 32, pp. 768–771, May 1996.
[7] O. C. Zienkiewicz, *The Finite Element Method*, 3rd ed. New York: McGraw-Hill, 1977.
[8] G. Dhatt and G. Touzot, *Une Présentation de la Méthode des Éléments Finis*, 2nd ed. Paris, France: Maloine SA, 1984.
[9] N. Beaudet, Ph.D. dissertation, University of Caen, 1997.
[10] T. Van Duzer and C. W. Turner, *Principle of Superconductive Devices and Circuits*. Edward Arnold, 1982.
[11] L. H. Lee, T. P. Orlando, and W. G. Lyons, "Current distribution in superconducting thin-film strips," *IEEE Trans. Appl. Superconduct.*, vol. 4, pp. 41–44, Mar. 1994.
[12] P. A. Rosenthal, M. R. Beasley, K. Char, M. S. Colclough, and G. Zaharchuk, "Flux focusing effects in planar thin film grain boundary Josephson junctions," *Appl. Phys. Lett.*, vol. 59, pp. 3482–3484, 1991.
[13] M. B. Ketchen, W. J. Gallagher, A. W. Kleinsasser, S. Murphy, and J. R. Clem, "DC SQUID flux focuser," *SQUID'85—Superconducting Quantum Interference Devices and Their Applications*. Walter de Gruyter, 1985.
[14] K. Suzuki and Y. Okabe, "Optimization of a dc SQUID magnetometer to minimize the field resolution," *IEEE Trans. Appl. Superconduct.*, vol. 5, pp. 2172–2175, 1995.

Christophe Cordier received the Engineer degree from the ISMRA-ENSI de Caen in 1997. He is currently pursuing the Ph.D. degree in electrical engineering at the Université de Caen.

His research interests include the study and modeling of superconducting devices.

Stéphane Flament received the Engineer degree from the ISMRA-ENSI de Caen in 1991 and the Ph.D. degree from the Université de Caen in 1994, both in electrical engineering.

He is a Lecturer at the ISMRA in the Electrical Engineering Department. His research interests include high Tc low noise superconducting magnetometers, including device modeling and default analysis.

Christian Dubuc received the Engineer degree from the ISMRA-ENSI, Caen, France, in 1968, and the Ph.D. degree from the Université of Caen, France, in 1972, both in electrical engineering.

He spent two years at Philips Components Research Laboratory of Caen, working in the area of semiconductors nuclear detectors. After leaving Philips and spending six years at the ISMRA of Caen, he joined in 1978 the University of Caen, where he is a Professor in the Departement of Physics and Electrical Engineering. His research interests include superconducting sensors and circuits with an emphasis on high-temperature superconducting devices modeling.